An Implicit Monte Carlo Method for Rarefied Gas Dynamics I: The Space Homogeneous Case.

Lorenzo Pareschi *
Russel E. Caflisch †

Abstract

For the space homogeneous Boltzmann equation, we formulate a hybrid Monte Carlo method that is robust in the fluid dynamic limit. This method is based on an analytic representation of the solution over a single time step and involves implicit time differencing derived from a suitable power series expansion of the solution (a generalized Wild expansion). A class of numerical schemes is obtained by substituting a Maxwellian distribution in place of the high order terms in the expansion. The numerical solution is represented as a convex combination of a non-equilibrium particle distribution and a Maxwellian. The hybrid distribution is then evolved by Monte Carlo with implicit time discretization. Computational simulations of spatially homogeneous problems by our method are presented here for the Kac model and for the Variable Hard Sphere model (including Maxwell molecules). Comparison to exact solutions and to Direct Simulation Monte Carlo (DSMC) computations show the robustness and the efficiency of the new method.

Key Words: Boltzmann equation, Monte-Carlo methods, fluid dyanmic limit, implicit time discretizations.

AMS (MOS) subject classifications: 76P05, 82C80, 65C05, 34A65.

*Mathematics Department, University of Ferrara. Email: pareschi@dm.unife.it.
†Mathematics Department, UCLA. Email: caflisch@math.ucla.edu. Research supported in part by the NSF through grants number DMS-9623087 and INT-9512772

1 Introduction

Computation for rarefied gas dynamics (RGD) in engineering applications is most frequently performed using Monte Carlo methods. The Direct Simulation Monte Carlo (DSMC) method [1] has been particularly successful for a wide range of applications, from the space shuttle to vacuum pumps [17, 18, 24]. Intermolecular collisions are the dominant feature of these particle methods, and the natural time scale for them is the collisional time.

This presents a difficulty for rarefied flows that are near to the fluid dynamic limit, since then the collisional time is very small. On the other hand, for such problems the actual time scale for evolution is the fluid dynamic time scale, which may be much larger than a collisional time. A nondimensional measure of the significance of collisions is given by the Knudsen number ε, which is small in the fluid dynamic limit and large in the free streaming limit. For small Knudsen numbers, existing Monte Carlo methods lose their efficiency because they operate on a much shorter time scale than is necessary.

The aim of this paper is to introduce a new Monte Carlo method that is robust in the fluid dynamic limit, by which we mean that it is accurate and efficient for a full range of Knudsen numbers. In this method, the molecular density function is represented as a sum of two pieces: a continuous density function and a discrete collection of particles. This representation allows implicit discretization for the time evolution of the Boltzmann equation, so that small Knudsen number ε does not require small time steps. In this way, the method automatically takes advantage of the fluid dynamic description for the evolution when this is appropriate and naturally makes the transition from RGD to fluid mechanics.

For transport theory in general, the problem of finding numerical methods that perform robustly in the fluid dynamic or diffusion limit is one of the most important computational challenges. Our work follows a line of related methods for other transport problems: Larsen and co-workers [3] were the first to develop robust methods for neutron transport in diffusive regimes. Similar results were derived by Jin and Levermore [11, 12] and recently by Naldi and Pareschi [19] and Jin, Pareschi and Toscani [13, 14]. Caflisch, Jin and Russo [5] developed a robust method for the Broadwell model of RGD.

Most recently, Gabetta, Pareschi, and Toscani [9] developed a robust method for the Boltzmann equation based on implicit time differencing derived from a suitable power series expansion, called Wild sum [25], which greatly influenced the present work. All of these methods were for finite difference or finite element type methods.

In a related paper, Pareschi and Russo [21] have developed a similar method based on a density function that is represented only by particles. This has the virtue of greatly simplifying the convection step. The hybrid method presented in the present paper is an improvement over this particle method both in accuracy and efficiency. It

combines a Monte Carlo algorithm for the particle fraction of the distribution together with a deterministic evolution of the continuous fraction. A brief description of both methods was presented in [20].

These are the first particle methods of this type. The only previous implicit version of a Monte Carlo method in transport problems was for the linear equation of photon transport [10].

Previous efforts to find hybrid methods by combining particle methods in some region of space and fluid methods in another were developed in [4]. Another related method [8] includes multiple collisions of some particles to improve the accuracy in each time step.

The numerical solution of the Boltzmann equation is usually approached by means of a splitting in time of convection and interactions between particles. In this paper, the method is developed only for the spatially homogeneous problem. In other words, the collisional step is included, but the convective step is not. Similarity solutions [16] in velocity and time are the main test problem here. The computations are performed using both the Kac model [15] and the Variable Hard Sphere models [2] including Maxwell molecules. In future work, for which we already have preliminary results, we will generalize this method to include spatial dependence, i.e. convection. This will be performed first for one dimension, on problems such as shock waves and flow between two plates, then for two dimensional problems, such as flow around an obstacle.

In the next section we recall some basic properties of the homogeneous Boltzmann equation and its time discretization. In Section 3 we discuss the time transformation from [9] that leads to implicit time differencing and the Wild sum formulation for the collision process. Then we introduce a class of schemes, which are robust in the fluid limit, based on replacing the high order terms in the Wild sum by a Maxwellian, i.e. relaxing them to equilibrium. In Section 4, we formulate an analytic representation of the particle density function f as a Maxwellian M plus another density function g, i.e. $f = (1-\beta)g + \beta M$ with $0 \leq \beta \leq 1$. We find equations for the evolution of β and g, which show how the solution evolves toward a Maxwellian distribution with $\beta = 1$.

A Monte Carlo method corresponding to this analytic representation is presented in Section 5. It is implemented for the Kac and VHS models in that section. Then computational results are presented in Section 6. Finally, a summary and discussion of future directions are presented in Section 7.

2 The space homogeneous Boltzmann equation

The spatially homogeneous Boltzmann equation is [6]

$$\frac{\partial f}{\partial t} = \frac{1}{\varepsilon} Q(f, f) \tag{1}$$

supplemented with the initial condition

$$f(v, t = 0) = f_0(v), \tag{2}$$

where $f = f(v,t)$ is a non negative function describing the time evolution of the distribution of particles which move with velocity v at time $t > 0$. The parameter $\varepsilon > 0$ is called the Knudsen number and is proportional to the mean free path between collisions. The bilinear collision operator $Q(f,f)$ describes the binary collisions of the particles and is given by

$$Q(f,f)(v) = \int_{I\!R^3} \int_{S^2} \sigma(|v - v_1|, \omega)[f(v')f(v'_*) - f(v)f(v_*)]\, d\omega\, dv_*. \tag{3}$$

In the above expression, ω is a unit vector of the sphere S^2, so that $d\omega$ is an element of area of the surface of the unit sphere S^2 in $I\!R^3$. Moreover (v', v'_*) represent the post-collisional velocities associated with the pre-collisional velocities (v, v_*) and the collision parameter ω; i.e.,

$$v' = \frac{1}{2}(v + v_* + |v - v_*|\omega), \quad v'_* = \frac{1}{2}(v + v_* - |v - v_*|\omega). \tag{4}$$

The kernel σ is a nonnegative function which characterizes the details of the binary interactions. In the case of inverse k-th power forces between particles the kernel has the form

$$\sigma(|v - v_*|, \theta) = b_\alpha(\theta)|v - v_*|^\alpha, \tag{5}$$

where $\alpha = (k-5)/(k-1)$. For numerical purposes, a widely used model is the Variable Hard Sphere(VHS) model [2], corresponding to $b_\alpha(\theta) = C_\alpha$ where C_α is a positive constant. The case $\alpha = 0$ is referred to as Maxwellian gas whereas the case $\alpha = 1$ yields the Hard Sphere gas.

During the evolution process, mass, momentum and energy are conserved; i.e.,

$$\int_{I\!R^3} Q(f,f)\phi(v)\, dv = 0, \quad \phi(v) = 1, v, v^2, \tag{6}$$

and in addition the distribution function f satisfies Boltzmann's well-known H-theorem

$$\frac{d}{dt}\int_{I\!R^3} f \log(f) dv \leq 0. \tag{7}$$

¿From a physical point of view, Boltzmann's H-theorem implies that any equilibrium distribution function, i.e. any function f for which $Q(f,f) = 0$, has the form of a locally Maxwellian distribution

$$M(\rho, u, T)(v) = \frac{\rho}{(2\pi T)^{3/2}} \exp(-\frac{|u - v|^2}{2T}), \tag{8}$$

where ρ, u, T are the density, mean velocity and temperature of the gas. From (6) it follows that these quantities do not vary with time, and hence we can write

$$\rho(t) = \int_{\mathbf{R}^3} f(v,t)\,dv = \rho(0), \tag{9}$$

$$u(t) = \frac{1}{\rho}\int_{\mathbf{R}^3} v f(v,t)\,dv = u(0), \tag{10}$$

$$T(t) = \frac{1}{3\rho}\int_{\mathbf{R}^3} [v-u(t)]^2 f(v,t)\,dv = T(0). \tag{11}$$

When the collisional time ε is small, then the problem (1) becomes stiff. A direct, explicit method such as DSMC then becomes computationally expensive, requiring time steps of size ε. An implicit method, on the other hand, would allow larger time steps by capturing the correct relaxation of the distribution f to Maxwellian. As discussed in the Introduction, the main point of this paper is to formulate an implicit particle method for the Boltzmann equation.

3 Implicit time discretizations

As proposed in [9], a general idea for deriving robust numerical schemes, by which we mean schemes that are unconditionally stable and preserve the asymptotics of the fluid dynamic limit, for a nonlinear equation like (1) is to replace high order terms of a suitable well-posed power series expansion by the local equilibrium. The great advantage of these implicit schemes is to be explicitely implementable.

Here we will first derive the schemes as presented in [9] and then we will show how it is possible to generalize this approach.

3.1 Wild sums expansions

Let us consider a differential system of the type

$$\frac{\partial f}{\partial t} = \frac{1}{\varepsilon}\left[P(f,f) - \mu f\right] \tag{12}$$

with the same initial condition (2) and where $\mu \neq 0$ is a constant and P a bilinear operator.

Let us replace the time variable t and the function $f = f(v,t)$ using the equations

$$\sigma = (1 - e^{-\mu t/\varepsilon}), \qquad F(v,\sigma) = f(v,t)e^{\mu t/\varepsilon}. \tag{13}$$

Then F is easily shown to satisfy

$$\frac{\partial F}{\partial \sigma} = \frac{1}{\mu}P(F,F) \tag{14}$$

with $F(v, \sigma = 0) = f_0(v)$.

Now, the solution to the Cauchy problem for (14) can be sought in the form of a power series

$$F(v, \sigma) = \sum_{k=0}^{\infty} \sigma^k f_k(v), \qquad f_{k=0}(v) = f_0(v) \tag{15}$$

where the functions f_k are given by the recurrence formula

$$f_{k+1}(v) = \frac{1}{k+1} \sum_{h=0}^{k} \frac{1}{\mu} P(f_h, f_{k-h}), \quad k = 0, 1, \ldots \tag{16}$$

Making use of the original variables we obtain the following formal representation of the solution to the Cauchy problem (1)

$$f(v, t) = e^{-\mu t/\varepsilon} \sum_{k=0}^{\infty} \left(1 - e^{-\mu t/\varepsilon}\right)^k f_k(v). \tag{17}$$

Remark 3.1 The method was originally developed by Wild [25] to solve the Boltzmann equation for Maxwellian molecules. Here we describe the method under more general hypothesis on P as derived in [9]. We emphasize that the representation (17) is not unique and other well-posed power series expansion can be obtained in a similar way [9].

Finally, note that expansion (17) continues to hold also if μ is a function of v. Unfortunately this choice leads to nonconservative schemes.

3.2 Truncation and time relaxed schemes

Now, we describe the numerical approximation to problem (14).

First, we state the following [9]

Proposition 3.1 *Let $P(f, f)$ be a nonnegative bilinear operator such that there exist some functions $\phi(v)$ with the following property*

$$\int_{I\!R^3} P(f, f)\phi(v)\, dv = \mu \int_{I\!R^3} f\, \phi(v)\, dv, \tag{18}$$

where $\mu > 0$. Then the coefficients $f^{(k)}$ defined by (16) are nonnegative and satisfy $\forall\, k > 0$

$$\int_{I\!R^3} f^{(k)}\phi(v)\, dv = \int_{I\!R^3} f^{(0)}\phi(v)\, dv. \tag{19}$$

Now, suppose the sequence $\left\{f^{(k)}\right\}_{k\geq 0}$ defined by (16) is convergent. Then (17) is well defined for any value of the mean free path. Moreover, if we denote by

$$M(v) = \lim_{k\to\infty} f_k \tag{20}$$

then

$$\lim_{t\to\infty} f(v,t) = M(v),$$

in which $M(v)$ is the local (Maxwellian) equilibrium.

In [9] the following class of numerical schemes, based on a suitable truncation for $m \geq 1$ of (17), has been constructed

$$f^{n+1}(v) = e^{-\mu\Delta t/\varepsilon} \sum_{k=0}^{m} \left(1 - e^{-\mu\Delta t/\varepsilon}\right)^k f_k^n(v) + \left(1 - e^{-\mu\Delta t/\varepsilon}\right)^{m+1} M(v), \tag{21}$$

where $f^n(v) = f(v, n\Delta t)$ and Δt is a small time interval.

The main reason for introducing these schemes is given by the following result [9]

Theorem 3.1 *The time discretization defined by (21) satisfies the following properties:*

i) If $\sup_{k>n}\{|f^{(k)} - M|\} \leq C$ *for a constant* $C = C(v)$*, then it is at least a m-order approximation (in* $\mu\Delta t/\varepsilon$*) of (17).*

ii) Under the same assumptions of Proposition 3.1, $f^{n+1}(v)$ *is nonnegative independently of the value of* ε *and satisfies*

$$\int_{I\!R^3} f^{n+1}\,\phi(v)\,dv = \int_{I\!R^3} f^n \phi(v)\,dv. \tag{22}$$

iii) For any $m \geq 1$*, we have*

$$\lim_{\varepsilon/(\mu\Delta t)\to 0} f^{n+1}(v) = M(v).$$

Remark 3.2 The previous theorem guarantees that the truncated sum (21) has the correct asymptotic behavior when $\varepsilon \to 0$. Clearly the accuracy of this approximation is related to the the rate of convergence of the sequence f_k towards $M(v)$. Finally we point out the fact that other truncations of (17) may be considered. For example, consider the approximation

$$f^{n+1}(v) = e^{-\mu\Delta t/\varepsilon} \sum_{k=0}^{m} \left(1 - e^{-\mu\Delta t/\varepsilon}\right)^k f_k^n(v) + \left(1 - e^{-\mu\Delta t/\varepsilon}\right)^{m+1} f_{m+1}^n(v). \tag{23}$$

It is easy to check that once again points (i) and (ii) hold also for (23). When the relaxation parameter ε is small,however, the accuracy of the approximation deteriorates dramatically, since the truncation does not possess the correct asymptotic limit.

3.3 Application to the Boltzmann equation

Now we apply the previous general approach to the Boltzmann equation and related kinetic models. To this aim, we will assume that the collision kernel satisfies a cut-off hypothesis.

Denote $Q_\Sigma(f,f)$ to be the collision operator obtained by replacing the kernel σ with the kernel σ_Σ

$$\sigma_\Sigma(|v-v_*|,\omega) = \min\{\sigma(|v-v_*|,\omega),\Sigma\}, \quad \Sigma > 0.$$

Thus, for a fixed Σ, let us consider the homogeneous problem

$$\frac{\partial f}{\partial t} = \frac{1}{\varepsilon} Q_\Sigma(f,f). \tag{24}$$

Problem (24) can be written in the form (12) taking

$$P(f,f) = Q_\Sigma^+(f,f) + f(v)\int_{I\!R^3}\int_{S^2}[\Sigma - \sigma_\Sigma(|v-v_*|,\omega)]f(v_*)\,d\omega\,dv_*, \tag{25}$$

with $\mu = 4\pi\Sigma\rho$ and

$$Q_\Sigma^+(f,f,) = \int_{I\!R^3}\int_{S^2}\sigma_\Sigma(|v-v_*|,\omega)f(v')f(v'_*)\,d\omega\,dv_*. \tag{26}$$

It is a simple exercise to verify that Proposition 3.1 holds with $\phi(v) = 1, v, v^2$. Since the coefficients $f_k(v)$, $k \geq 1$, of expansion (16), include numerous five fold integral like (25), the most efficient scheme for practical applications is that for $m = 1$.

This scheme provides a first order approximation to the solution by substituting $f_k, k \geq 2$ with the local Maxwellian (8).

With the notations of the previous sections, the first order scheme reads

$$f^{n+1}(v) = (1-\tau)f^n(v) + \tau(1-\tau)f_1^n(v) + \tau^2 M(v), \tag{27}$$

where $\tau = \left(1 - e^{-\mu\Delta t/\varepsilon}\right)$. The results of the last two subsections show that the approximation defined by (27) is well-defined independently of the Knudsen number, has the correct moments, and converges towards the correct fluid-dynamic limit.

The time relaxed approximation can generally be written in the form

$$f^{n+1}(v) = A(\lambda)f^n(v) + B(\lambda)f_1^n(v) + C(\lambda)M(v) \tag{28}$$

where $\lambda = \mu\Delta t/\varepsilon$ and the weights A, B and C are nonnegative functions. For conservation we must have

$$A(\lambda) + B(\lambda) + C(\lambda) = 1, \quad \forall\,\lambda, \tag{29}$$

A choice of functions which satisfies the previous requirements is given by

$$A = 1-\tau, \quad B = \tau(1-\tau), \quad C = \tau^2, \tag{30}$$

which corresponds to the scheme (27). A better choice of parameters is [20]

$$A = 1 - \tau, \quad B = \tau(1 - \tau^2), \quad C = \tau^3, \tag{31}$$

which corresponds to taking $f_2 = f_1$, $f_k = M$, $k \geq 3$ in (17).

Remark 3.3 In some particular situations the method is considerably simplified.

- For the one-dimensional Kac equation [15],

$$\frac{\partial f}{\partial t} = \frac{1}{\varepsilon} \int_{-\infty}^{+\infty} \frac{1}{2\pi} [f(v')f(v'_*) - f(v)f(v_*)]\, dv_*\, d\theta \tag{32}$$

  where

$$v' = v\cos\theta - v_* \sin\theta, \qquad v'_* = v\sin\theta + v_*\cos\theta, \tag{33}$$

  the previous scheme can be applied directly taking

$$P(f,f) = \frac{1}{2\pi} \int_{-\infty}^{+\infty} f(v')f(v'_*)\, dv_*\, d\theta, \tag{34}$$

  and $\mu = \rho$.

  Since, the only conserved quantities are the total mass and the energy, Proposition 3.1 holds for $\phi(v) = 1, v^2$.

- For Maxwell molecules the situation is similar to the case of Kac equation. In fact, since the collision kernel does not depend on the relative velocity $\sigma_\Sigma = \sigma_\Sigma(\omega)$ we simply have $P(f,f) = Q^+_\Sigma(f,f)$ and $\mu = \rho\bar{\sigma}$ where

$$\bar{\sigma} = \int_{S^2} \sigma_\Sigma(\omega) d\omega. \tag{35}$$

4 Splitting of the Maxwellian part

In this section, we formulate an analytic representation for the density function f which takes advantage of the relaxed time discretization presented in the previous section. In the next section the analytic representation will be translated into a numerical representation. Specifically one of the components of f will be replaced by a discrete set of particles.

As derived in the previous section, the general form for a single step of the Wild relaxed time discretization is

$$f^{n+1} = Af^n + Bf_1^n + CM \tag{36}$$

in which f^n is the density function at time step n, $f_1^n = P(f^n, f^n)/\mu$ is the first order term in (17) and the coefficients A, B, C are positive constants as in the previous section.

In order to analyze and exploit the discretization (36), write f as the linear combination of a Maxwellian density and a non-Maxwellian density, as

$$f^n(v) = (1 - \beta^n) g^n(v) + \beta^n M(v) \tag{37}$$

in which β is a nonnegative scalar. The Maxwellian density M is chosen to have the same macroscopic parameters as f^n, i.e.

$$\rho_M = \rho_f, \quad u_M = u_f, \quad T_M = T_f, \tag{38}$$

which is equivalent to

$$\int_{\mathbb{R}^3} \phi(v) f(v) dv = \int_{\mathbb{R}^3} \phi(v) M(v) dv, \tag{39}$$

with $\phi(v) = 1, v, v^2$.

In (38) and (39) we have omitted the superscript n, since ρ_f, u_f and T_f are independent of n, and as a result M is independent of n.

Now insert the representation (37) for f^n into the discretization (36) and use the fact that

$$f_1(M, M) = M. \tag{40}$$

The right hand side of (36) then naturally splits into a Maxwellian part $\beta^{n+1} M$ and a non-Maxwellian part $(1 - \beta^{n+1}) g^{n+1}$, in which

$$\beta^{n+1} = A\beta^n + B(\beta^n)^2 + C \tag{41}$$

$$\begin{aligned} (1 - \beta^{n+1}) g^{n+1} = {} & A(1 - \beta^n) g^n + B(1 - \beta^n)^2 f_1(g^n, g^n) \\ & + 2B(1 - \beta^n)\beta^n f_1(g^n, M). \end{aligned} \tag{42}$$

It follows that

$$g^{n+1} = (A + B(1 + \beta^n))^{-1} \left(A g^n + B(1 - \beta^n) f_1(g^n, g^n) + 2B\beta^n f_1(g^n, M) \right). \tag{43}$$

Equation (41) is an iterated map for the coefficient β and can be rewritten using the conservation property (29) as

$$\beta^{n+1} - \beta^n = B(\beta^n - 1)(\beta^n - C/B). \tag{44}$$

This discrete dynamical system has stationary points $\beta = 1$ and $\beta = C/B$. Our interest is only in $0 \leq \beta \leq 1$, which is an invariant region for the system. Hence we can state the following results:

Proposition 4.1 *i) If $C/B > 1$, then $\beta = 1$ is an attracting point and $\beta^n \to 1$ as $n \to \infty$ at an exponential rate with coefficient $(C - B)$, i.e.*

$$1 - \beta^n \cong \alpha(C - B)^n, \quad \alpha \neq 0, \tag{45}$$

for n large, if $C/B > 1$.

ii) If $C/B < 1$, then $\beta = 1$ is unstable and $\beta = C/B$ is attracting. In this case $\beta^n \to C/B$ as $n \to \infty$ at an exponential rate with coefficient $(B - C)$, i.e.

$$|C/B - \beta^n| \cong \alpha(B - C)^n, \quad \alpha \neq 0, \tag{46}$$

for n large, if $C/B < 1$.

Remark 4.1 The requirement $C/B > 1$ cannot be verified uniformly in $\lambda = \mu\Delta t/\epsilon$. However, the fluid regime corresponds to $\lambda \gg 1$ so that $C/B \gg 1$ because of the asymptotic preserving property. This shows that β^n increases monotonically to 1 in the fluid region, as desired.

For example, for the first order scheme corresponding to (30), $C/B = \tau/(1 - \tau)$. It follows that $\beta^n \to 1$ if $\tau > 1/2$. Similarly the scheme characterized by (31) has $C/B = \tau^2/(1 - \tau^2)$. Hence $\beta^n \to 1$ if $\tau > 1/\sqrt{2}$.

Clearly, near the fluid limit $\mu\Delta t/\varepsilon \gg 1$ and hence $\tau = 1 - e^{-\mu\Delta t/\varepsilon} \approx 1$.

5 Hybrid time relaxed Monte Carlo methods

In this section we describe the Monte Carlo method for the evolution of the density function f.

We develop the algorithms first in the simple case of constant cross sections (Kac equation and Maxwellian molecules) and then for the Boltzmann equation for Variable Hard Sphere gas.

5.1 Formulation of the method

Here we describe our new algorithm based on the evolution of the mixed distribution $f = (1-\beta)g+\beta M$. As described in Section 4, the distinguishing feature of our method is that the Maxwellian part of the distribution is represented analytically and the non Maxwellian fraction is represented as a particle distribution; i.e.,

$$f^n(v) = (1 - \beta^n)g^n(v) + \beta M(v), \tag{47}$$

in which

$$g^n(v) = \frac{1}{N_n}\sum_{i=1}^{N_n} \delta(v - v_i^n). \tag{48}$$

Our starting point is the evolution equation (42) for g^n, which can be written as

$$g^{n+1} = p_1 g^n + p_2 \left[q_1 \frac{P(g^n, g^n)}{\mu} + q_2 \frac{P(g^n, M)}{\mu} \right], \tag{49}$$

in which

$$p_1 = \frac{A}{A + B(1+\beta^n)}, \quad p_2 = \frac{B(1+\beta_n)}{A + B(1+\beta_n)}, \tag{50}$$

$$q_1 = \frac{1-\beta^n}{1+\beta^n}, \quad q_2 = \frac{2\beta^n}{1+\beta^n}. \tag{51}$$

Note that if f^n is a probability density, so is g^n. Moreover, $p_1 \geq 0$, $p_2 \geq 0$, $p_1 + p_2 = 1$, $q_1 \geq 0$, $q_2 \geq 0$, $q_1 + q_2 = 1$, and therefore p_1 and p_2 can be interpreted as probabilities, and q_1 and q_2 can be interpreted as conditional probabilities.

Therfore, Eq. (49) has the following probabilistic interpretation: a particle extracted from g^n has no collision with probability p_1, it collides with another particle extracted from g^n with probability $p_2 q_1$, or it collides with a particle sampled from the Maxwellian with probability $p_2 q_2$.

Note that this probabilistic interpretation is uniformly valid in $\mu\Delta t/\epsilon$. Moreover as $\mu\Delta t/\epsilon \to \infty$, $\beta^n \to 1$ because of the asymptotic preserving property of the quantities A, B and C. Therefore the density function f^n has the correct fluid limit.

The above interpretation suggests a Monte Carlo algorithm for the evolution of the distribution $f^n = (1-\beta^n) g^n + \beta^n M$.

Remark 5.1 If the number of particles is kept fixed, then their weight changes, since the mass associated to the particles is proportional to $(1-\beta^n)$. Instead, we chose to use a variable number of particles with constant weight per particle. This choice has several advantages. It improves the efficiency of the method, since the number of particles (and hence the computational cost) decreases without affecting the accuracy, and it simplifies the exchange of particles between cells in a spatially inhomogeneous problem.

5.2 Maxwellian molecules

We first describe the method when $P(f,f) = Q^+(f,f)$. In this case, a Monte Carlo algorithm based on Eq. (42),(49–51) is given by

Algorithm 5.1 :

1. *set M to be the Maxwellian with the same moment as the original distribution f_0*
2. *start with N_0 particles sampled from $f_0(v)$, and set $\beta^0 = 0$*
3. *compute $A(\mu\Delta t/\epsilon), B(\mu\Delta t/\epsilon), C(\mu\Delta t/\epsilon)$*

4. for $n = 10 \cdots n_{\text{tot}} - 1$

- $\beta^{n+1} = A\beta^n + B(\beta^n)^2 + C$
- *compute* p_1, p_2, q_1, q_2
- *compute the expected number of collision pairs:*
  - $N_{gg} = p_2 q_1 N_n/2$
  - $N_{gM} = p_2 q_2 N_n/2$
- *perform* N_{gg} *collisions between two g particles (exactly as in standard DSMC)*
- *perform* $2N_{gM}$ *collisions between a g particle and a Maxwellian*
  - *extract* i *without repetition*
  - *sample* v *from the Maxwellian* M *with the same moment as the original distribution* f^n
  - *perform the collision between* v_i *and* v
  - *assign* $v_i^{n+1} = v_i'$
- *update* N: $N_{n+1} = \text{Round}(N_0(1 - \beta_{n+1}))$
- *correct* β^{n+1} *in order to preserve mass:* $\beta_{n+1} = 1 - N_{n+1}/N_0$

Remark 5.2 The above scheme conserves momentum and energy only on the average, but not exactly. This is because the collisions with the Maxwellian M, if performed independently from each other, do not maintain exact conservation of momentum and energy. By taking this into account, a conservative algorithm can be constructed by changing momentum u_M and energy E_M of the Maxwellian fraction after each collision (*local conservation*), according to

$$u_M' = u_M - \frac{v_j' - v_j}{N^0 \beta^n}, \quad E_M' = E_M - \frac{(v_j')^2 - (v_j)^2}{2N^0 \beta^n}, \quad n > 0, \tag{52}$$

where

$$E_M = \frac{1}{2}(d\, T_M + u_M^2),$$

d is the dimension of the velocity space and T_M is the temperature of the Maxwellian.

Alternatively, conservation can be restored by modifying the moments associated to the Maxwellian fraction at the end of each time step (*global conservation*).

This is obtained by imposing

$$(1 - \beta^{n+1})E_p + \beta^{n+1} E_M = E^0, \quad (1 - \beta^{n+1})u_p + \beta^{n+1} u_M = u^0, \quad n > 0,$$

where u_p and E_p are the mean velocity and energy of the particles.

The two approaches give very similar results and can be used if β^n is not too small.

If the distribution is very far from equilibrium, i.e. if $\beta_n \ll 1$, then because of fluctuations, it may happen that the energy decreases too much, and it is impossible to change the parameters of the Maxwellian to impose conservation. On the other hand, in this case, only a very small fraction of collisions will be non conservative, and therefore the lack of exact conservation will not affect the quality of the result.

5.3 VHS kernels

Now we consider the case of VHS collision kernels. In this case the dynamics of the collision is locally characterized by the quantities $\tau_{ij} = \exp(-\sigma_{ij}\rho\Delta t/\epsilon)$ which depend on the pair. This gives rise to a local evolution of β^n.

An acceptance-rejection technique, similar to the one used for DSMC, can be adopted. The conservative algorithm to update β^n and g^n can be written as

Algorithm 5.2 :

1. *set* $\beta = 0, N_c = 0$
2. *compute an upper bound* Σ *of* σ_{ij} *(as in DSMC)*
3. *compute* $\tau = \exp(-\rho\Sigma\Delta t/\epsilon)$ *and the corresponding quantities* $A, B, C, p_1, p_2, q_1, q_2$
4. *compute the number of dummy collision pairs:*
   - $N_{gM} = p_2 q_2 N_n/2$
   - $N_{gg} = p_2 q_1 N_n/2$
5. *perform* N_{gg} *dummy collisions between g-particles, i.e.*
   - *extract* (i, j) *without repetition*
   - *compute* $A_{ij}, B_{ij}, C_{ij}, p_{2ij}$
   - *if* $p_2 \,\mathrm{Rand} < p_{2ij}$ *then perform the collision between* v_i *and* v_j *(as in standard DSMC)*
     - $\beta \leftarrow \beta + 2\beta_{ij}$
     - $N_c \leftarrow N_c + 2$
6. *perform* $2N_{gM}$ *dummy collisions between the g-particles and the Maxwellian,*
   - *extract* i *without repetition*
   - *sample one particle,* m*, from the Maxwellian*
   - *compute* $A_{im}, B_{im}, C_{im}, p_{2im}$
   - *if* $p_2 \,\mathrm{Rand} < p_{2im}$ *then perform the collision between* v_i *and the Maxwellian*

- $\beta \leftarrow \beta + \beta_{im}$
- $N_c \leftarrow N_c + 1$

7. $\beta^{n+1} = \beta / N_c$
8. *update* N: $N_{n+1} = \text{Round}(N_0(1 - \beta^{n+1}))$
9. *correct* β^{n+1} *in order to preserve mass*
10. *correct* u_M *and* T_M *to maintain conservation of momentum and energy.*

Remark 5.3 Note that in the space homogeneous case, the Maxwellian equilibrium fraction β^n can only increase, and, consequently, the number of particles can only decrease if we start from a a completely discrete distribution ($\beta^0 = 0$). When $N^{n+1} < N^n$, some particles are just disregarded. In accordance with the evolution equation for β, if $\Delta t/\epsilon$ is sufficiently large, the number of particles decreases exponentially, and the distribution is rapidly projected onto a Maxwellian.

6 Numerical Results

In this section we test the hybrid time relaxed Monte Carlo (TRMCH) by comparing it with standard DSMC. We consider three initial value problems, respectively for the Kac equation, Boltzmann equation for Maxwell molecules, and Hard Spheres. In our tests we use the set of parameters defined by (31) and perform a single run, with a number of particles sufficiently large to control the effects of the fluctuations. We express the results as a function of the scaled time variable t/ϵ which we denote again by t in order to simplify the notations.

6.1 The Kac equation

We compare the Monte Carlo solutions with an exact solution of the Kac equation (32), corresponding to the initial condition

$$f_0(v) = v^2 \exp(-v^2), \quad v \in I\!R.$$

The solution is given by [16]:

$$f(v,t) = \frac{1}{2}\left[\frac{3}{2}(1-C)\sqrt{C} + (3C-1)C^{3/2}v^2\right]\exp\left(-Cv^2\right),$$

where

$$C = \frac{1}{3 - 2\exp(-\sqrt{\pi}t/16)}.$$

In order to compare our results with those obtained in [8], we reconstruct the density function on a grid, by convolving the particle distribution by a suitable mollifier.

More precisely, we use

$$f_{DSMC}(V_I) = \frac{1}{N}\sum_{j=1}^{N} W_H(V_I - v_j), \tag{53}$$

$$f_{TRMCH}(V_I) = (1-\beta^n)\frac{1}{N^n}\sum_{j=1}^{N^n} W_H(V_I - v_j^n), + \beta^n M^n(V_I), \tag{54}$$

where f_{DSMC} and f_{TRMCH} denote, respectively, the reconstructed density function obtained by DSMC and TRMCH on a regular grid

$$\{V_I = V_{\min} + I\Delta V, I = 1, \ldots, N_g\}.$$

The smoothing function W_H is given by

$$W_H(x) = \frac{1}{H} W\left(\frac{x}{H}\right), \quad W(x) = \begin{cases} 3/4 - x^2 & \text{if } |x| \le 0.5, \\ (x-3/2)^2/2 & \text{if } 0.5 < |x| \le 1.5, \\ 0 & \text{otherwise.} \end{cases}$$

The value $H = 0.2$ has been selected as a good compromise between fluctuations and resolution. The simulations are performed for $t \in [0, 8]$ by starting with $N = 5\times 10^4$ particles.

In Fig. 1 we present the numerical results obtained with the same time step $\Delta t = 0.5$ at two different times. The corresponding L^2-norm of the error is reported in Fig. 3 (left).

It is evident that TRMCH gives a better representation of the solution especially near the local extrema.

Fig. 2 shows the results of the same test where the time step of the TRMCH is four times larger then the one used by DSMC. The L^2-norm of the error is plotted in in Fig. 3 (right). Note that in spite of the larger time step, TRMCH solution seems to better capture the features of the exact solution.

We remark that in the first test case (Fig. 1) the computational cost of TRMCH is slightly lower than the cost of DSMC, while in the second case (Fig. 2) it is about five times smaller. This is because for TRMCH the number of particles (and therefore the number of collision per time step) decreases in time (see Fig. 4).

6.2 Maxwell molecules

Next we consider the 2D homogeneous Boltzmann equation for Maxwell molecules. An exact solution of the equation corresponding to the initial condition

$$f_0(v) = \frac{v^2}{\pi}\exp\left(-v^2\right), \tag{55}$$

is given by

$$f(v,t) = \frac{1}{2\pi C}\left[1 - \frac{1}{C}(1-C)\left(1 - \frac{v^2}{2C}\right)\right]\exp\left(-\frac{v^2}{2C}\right), \tag{56}$$

where $C(t) = 1 - (1/2)\exp(-t/8)$.

The comparison with the exact solution is obtained by reconstructing the function on a regular grid of spacing $\Delta v = 0.25$ by the "weighted area rule".

All the simulations have been performed for $t \in [0, 16]$ by starting with $N = 10^5$ particles.

In Fig. 5 we show the L^2 norm of the error in time for both DSMC and TRMCH on the time interval [0,8]. In the first test we use the same time step $\Delta t = 0.4$. The results confirm the gain of accuracy of the TRMCH method on the transient time scale (left). For $t \geq 4$, the methods are almost equivalent since the maximum value reached by β^n at the end of the simulation is about 0.12 and hence most of the distribution is composed of particles.

Using a time step of $\Delta t = 0.6$ for the TRMCH and $\Delta t = 0.15$ for the DSMC the gain of accuracy is less evident but more uniform in time (right). Here the final value of β^n is about 0.25.

We report in Fig. 6 the variations of the moments associated to the Maxwellian fraction in the TRMCH method. The variation in the first time steps is due to the fact that we use, as initial moments of the hybrid distribution, the exact moments of the analytical solution.

Finally, we test the schemes by computing the fourth order moment in time and by comparing it with the exact solution

$$\mathcal{M}_4(t) = 8C(t)(2 - C(t)). \tag{57}$$

For the TRMCH method the we use relations

$$\mathcal{M}_4^{TRMCH} = (1-\beta^n)\frac{1}{N^n}\sum_{i=1}^{N^n}\delta(v - v_i)v_i^4 + \beta^n(8T_M^2 + u_M^2(8T_M + u_M^2)).$$

The results are plotted in Figs. 7. It is clear that the solution given by TRMCH is more accurate even with a larger time step.

6.3 VHS molecules

The last test problem deals with the numerical solution of the Boltzmann equation for Hard Sphere molecules (VHS, for $\alpha = 1$) with $C_\alpha = 1$.

The initial condition is the same used for the Maxwell molecules (55). The "exact" solution has been computed using the DSMC method with 2×10^6 particles and $\Delta t = 5 \times 10^{-3}$.

As in the previous case, the density distribution is obtained by reconstructing the function on a regular grid of spacing $\Delta v = 0.25$ by the "weighted area rule" and the simulations have been performed for $t \in [0, 16]$ by starting with $N = 10^5$ particles.

In Fig. 8 we show the time evolution of the fourth order moment of the solution. The results confirm the gain of accuracy and the reduction of fluctuations of the TRMCH method with respect to the DSMC method for larger time steps.

Next we report the number of dummy collisions and the number of effective collisions per time step performed by DSMC and TRMCH (Fig. 9).

In spite of the fact that the time step for TRMCH is larger than that of DSMC, the number of dummy collision is higher for DSMC. The reason is that this number is proportional to $\mu\Delta t$ for DSMC, and it is proportional to $1 - \exp(-\mu\Delta t)$ for TRMCH. This is an additional reason of the better efficiency of the TRMCH with respect to DSMC.

Finally we give in Fig. 10 the variations of β^n and of the number of particles in time for the TRMCH method.

7 Conclusion and future works

The implicit Monte Carlo method presented above has been shown to provide favorable performance for spatially homogeneous problems, in comparison to the DSMC method. Longer time steps are allowed, without degradation of accuracy, because of the implicit time discretization. In the small relaxation limit, the method projects the density distribution to the correct equilibrium state.

Computational complexity and statistical variance are reduced because of the smaller number of particles used to represent the solution, the remainder of which is represented by a continuous (Maxwellian) distribution. Both of these improvements are made possible by approximating the Boltzmann solution using a generalized Wild sum.

The spatially homogeneous problem is presented here mainly as a step towards a complete method for spatially inhomogeneous problems. In these problems, convection drives the distribution away from equilibrium while collisions drive it toward equilibrium. Although the new method has yet to be validated for spatially inhomogeneous problems, we have obtained some promising preliminary results. In particular we expect that the TRMCH method including convection will be robust in the fluid dynamic limit, allowing time steps on the fluid dynamic time scale and reducing to a kinetic scheme for the fluid equations [7, 22].

Previous attempts to obtain such a robust method have had only limited success. One of the main obstacles has been the difficulty of recognizing when a particle distribution is close to equilibrium or picking out the Maxwellian component of a distribution. Indeed for standard particle methods, there is no reduction in computational complexity when the distribution is at equilibrium. We believe that this difficulty has been

solved in the TRMCH method: The Maxwellian component of the distribution evolves according to a deterministic scheme derived from the generalized Wild sum.

A related paper [21] presents a simpler version of the method, simply called TRMC, in which the Maxwellian component is also represented by particles instead of by a continuous distribution. In each time step, the particles from the Maxwellian component are sampled directly from a Maxwellian distribution. This still allows longer time steps, since it involves implicit time discretization, but the fluctuations are not reduced. The generalization to spatial inhomogeneities is particularly straightforward for this method, since convection can be performed directly on the particles. In the fluid limit the method becomes a particle scheme for the Euler equations [23].

References

[1] G.A. Bird. Direct simulation and the Boltzmann equation. *Physics of Fluids A*, 13:2672–2681, 1970.

[2] G.A. Bird. *Molecular Gas Dynamics*. Oxford University Press, London, 1976.

[3] C. Borgers, E. W. Larsen, and M. L. Adams. The asymptotic diffusion limit of a linear discontinuous discretization of a two-dimensional linear transport equation. *Journal of Computational Physics*, 98:285–300, 1992.

[4] J.F Bourgat, P LeTallec, B. Perthame, and Y. Qiu. Coupling Boltzmann and Euler equations without overlapping. In *Domain Decomposition*. AMS, 1992.

[5] R. E. Caflisch, S. Jin, and G. Russo. Uniformly accurate schemes for hyperbolic systems with relaxation. *SIAM Journal on Numerical Analysis*, 34:246–281, 1997.

[6] C. Cercignani. *The Boltzmann Equation and its Applications*. Springer-Verlag, 1988.

[7] S. Deshpande. A second order accurate kinetic theory based method for inviscid compressible flow. *Journal of Computational Physics*, 1979.

[8] L. Desvillettes and R.E. Peralta Herrera. A vectorizable simulation method for the Boltzmann equation. *Mathematical Modeling and Numerical Analysis*, 28:745–760, 1994.

[9] E. Gabetta, L. Pareschi, and G. Toscani. Relaxation schemes for nonlinear kinetic equations. *SIAM Journal on Numerical Analysis*, 34:2168–2194, 1997.

[10] J.A. Fleck, Jr. and J.D. Cummings. An implicit Monte Carlo scheme for calculating time and frequency dependent nonlinear radiation transport. *Journal of Computational Physics*, 8:313–342, 1971.

[11] S. Jin and C. D. Levermore. Fully-discrete numerical transfer in diffusive regimes. *Transport Theory and Statistical Physics*, 22:739–791, 1993.

[12] S. Jin and C. D. Levermore. Numerical schemes for hyperbolic conservation laws with stiff relaxation terms. *Journal of Computational Physics*, 126:449–467, 1996.

[13] S. Jin, L. Pareschi, and G. Toscani. Diffusive relaxation schemes for multiscale discrete-velocity kinetic equations. *SIAM Journal on Numerical Analysis*, 35:2405–2439, 1998.

[14] S. Jin, L. Pareschi, and G. Toscani. Uniformly accurate diffusive relaxation schemes for transport equations. *SIAM Journal on Numerical Analysis*, 1998. submitted.

[15] M. Kac. Probability and related topics in physical sciences. In *Lectures in Applied Mathematics*. Interscience Publishers London-New York, 1957.

[16] M. Krook and T.T. Wu. *Physical Review Letters*, 36:107, 1976.

[17] J.N. Moss and J.M. Price. Direct simulation of AFE forebody and wake flow with thermal radiation. In *Rarefied Gas Dynamics: Theoretical and Computational Techniques, Progress in Aeronautics and Astronautics, 118*, pages 413–431. Proceedings of the 16th International Symposium on Rarefied Gas Dynamics, 1988.

[18] E.P. Muntz. Rarefied gas dynamics. *Annual Review of Fluid Mechanics*, 21:387–417, 1989.

[19] G. Naldi and L. Pareschi. Numerical schemes for kinetic equations in diffusive regimes. *Applied Mathematical Letters*, 11:29–35, 1998.

[20] L. Pareschi and G. Russo. Asymptotic preserving Monte-Carlo methods for the Boltzmann equation. *Transport Theory and Statistical Physics*, 1998. submitted.

[21] L. Pareschi and G. Russo. Time relaxed Monte-Carlo methods for the Boltzmann equation. 1998. preprint.

[22] B. Perthame. Boltzmann type schemes for gas dynamics and the entropy property. *SIAM Journal on Numerical Analysis*, 27:1405–1421, 1990.

[23] D.I. Pullin. Direct simulation methods for compressible inviscid ideal gas flow. *Journal of Computational Physics*, 1978.

[24] A.K. Rebrov. Studies on physical gas dynamics of jets as applied to vacuum pumps. In V. Boffi and C. Cercignani, editors, *Proceedings of the 15th International Symposium on Rarefied Gas Dynamics*, pages 455–473, 1986.

[25] E. Wild. On Boltzmann's equation in the kinetic theory of gases. *Proc. Camb. Phil. Soc.*, 47:602–609, 1951.

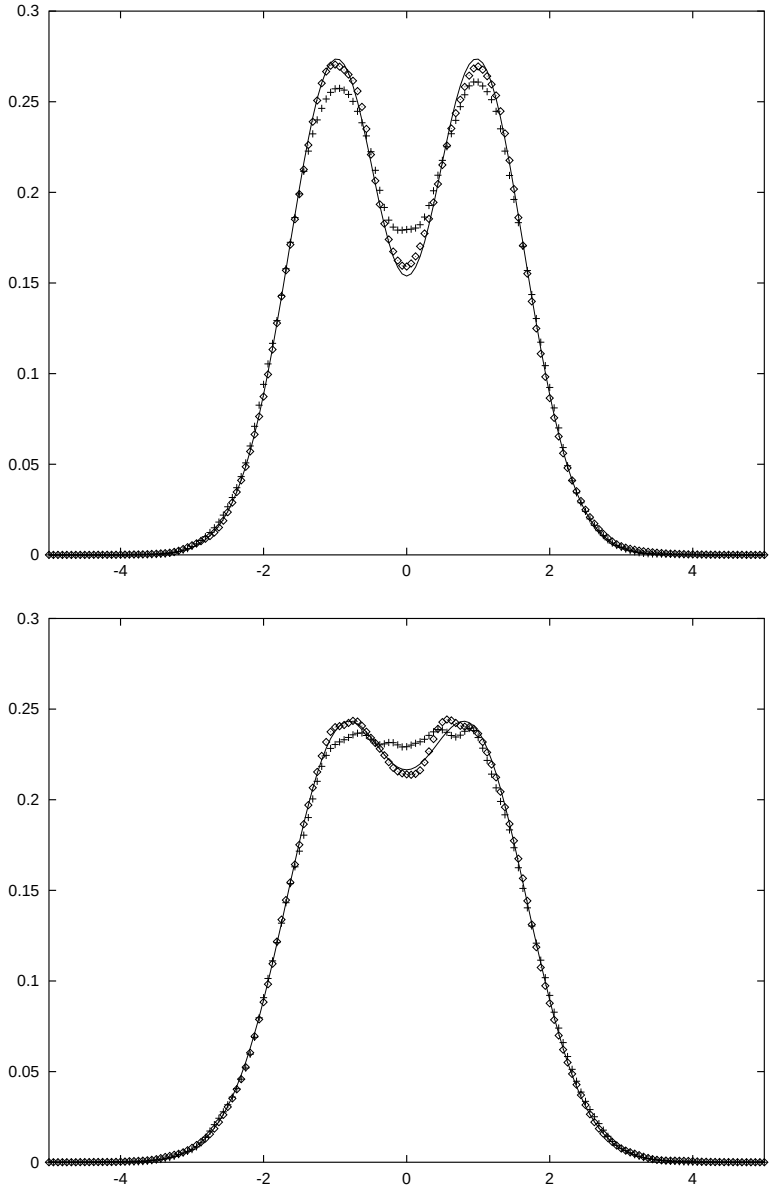

Figure 1: Kac equation: distribution function at time $t = 1.5$ (top) and $t = 3.0$ (bottom): Exact (line), DSMC (+) and TRMCH ($\diamond$). Time step $\Delta t = 0.5$

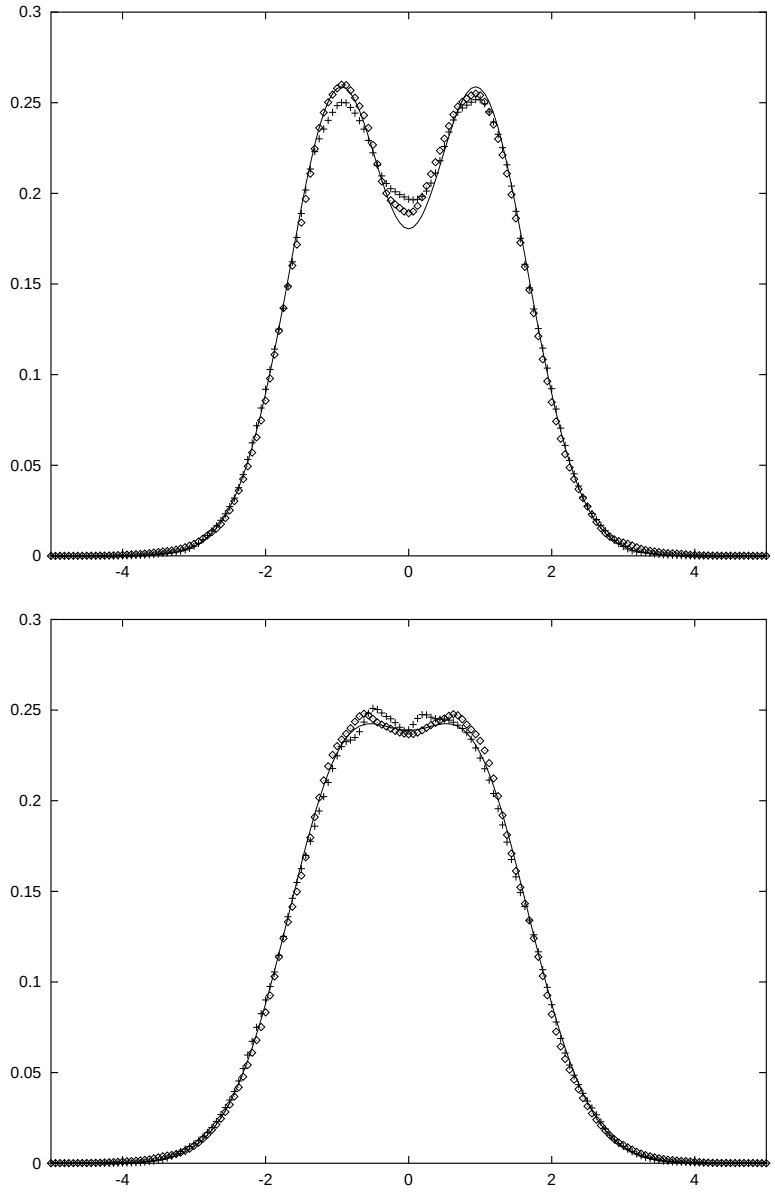

Figure 2: Kac equation: distribution function at time $t = 2.0$ (top) and $t = 4.0$ (bottom): Exact (line), DSMC ($+$) and TRMCH ($\diamond$). Time step: $\Delta t = 0.25$ (DSMC) and $\Delta t = 1.0$ (TRMCH)

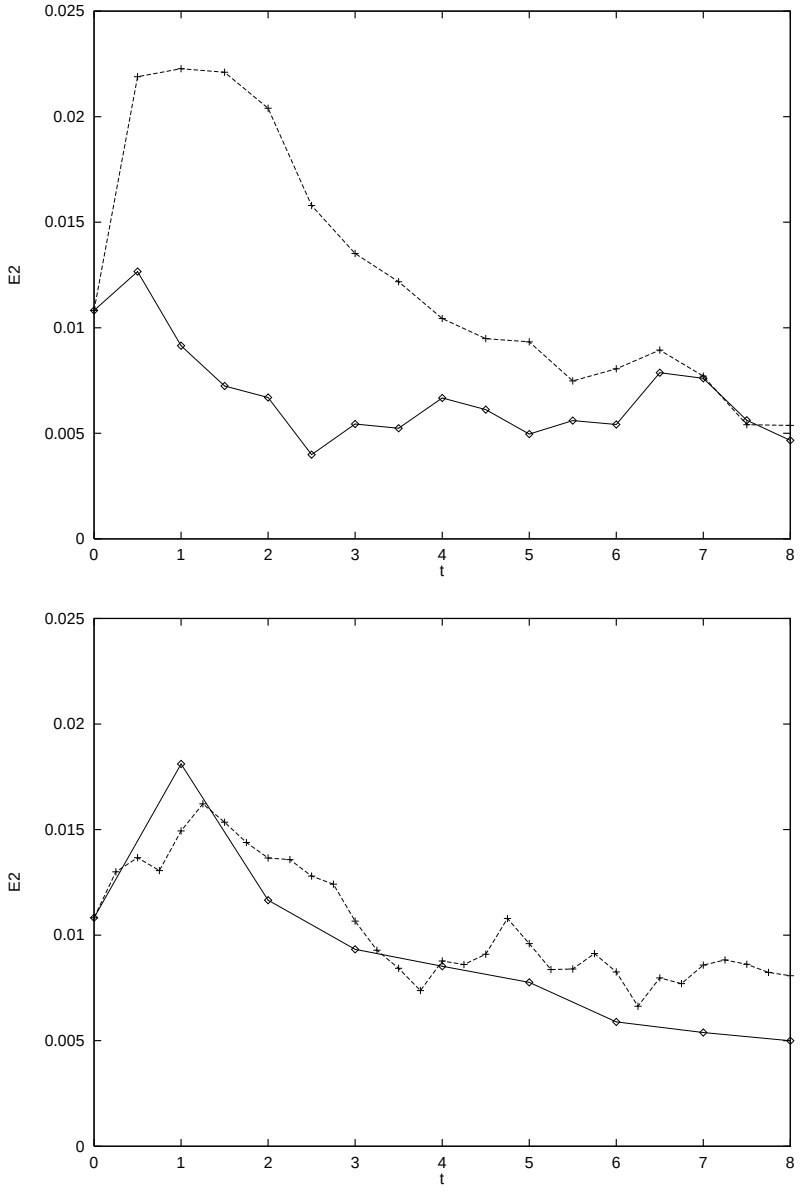

Figure 3: Kac equation: L^2 error vs time, DSMC (+) and TRMCH ($\diamond$). Top: $\Delta t = 0.5$. Bottom: $\Delta t = 0.25$ (DSMC), $\Delta t = 1.0$ (TRMCH).

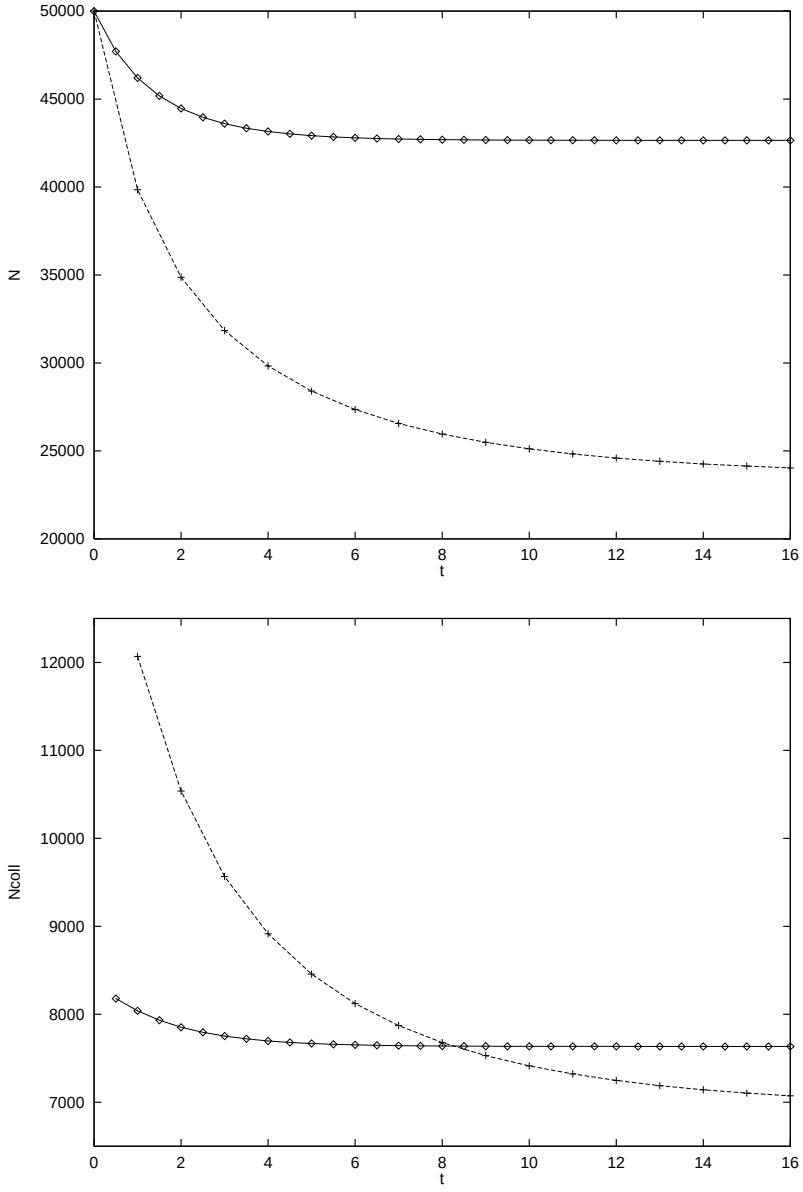

Figure 4: Kac equation: Number of particles (top) and number of collisions (bottom) vs time for TRMCH. Time step: $\Delta t = 0.5$ ($\diamond$), $\Delta t = 1.0$ ($+$).

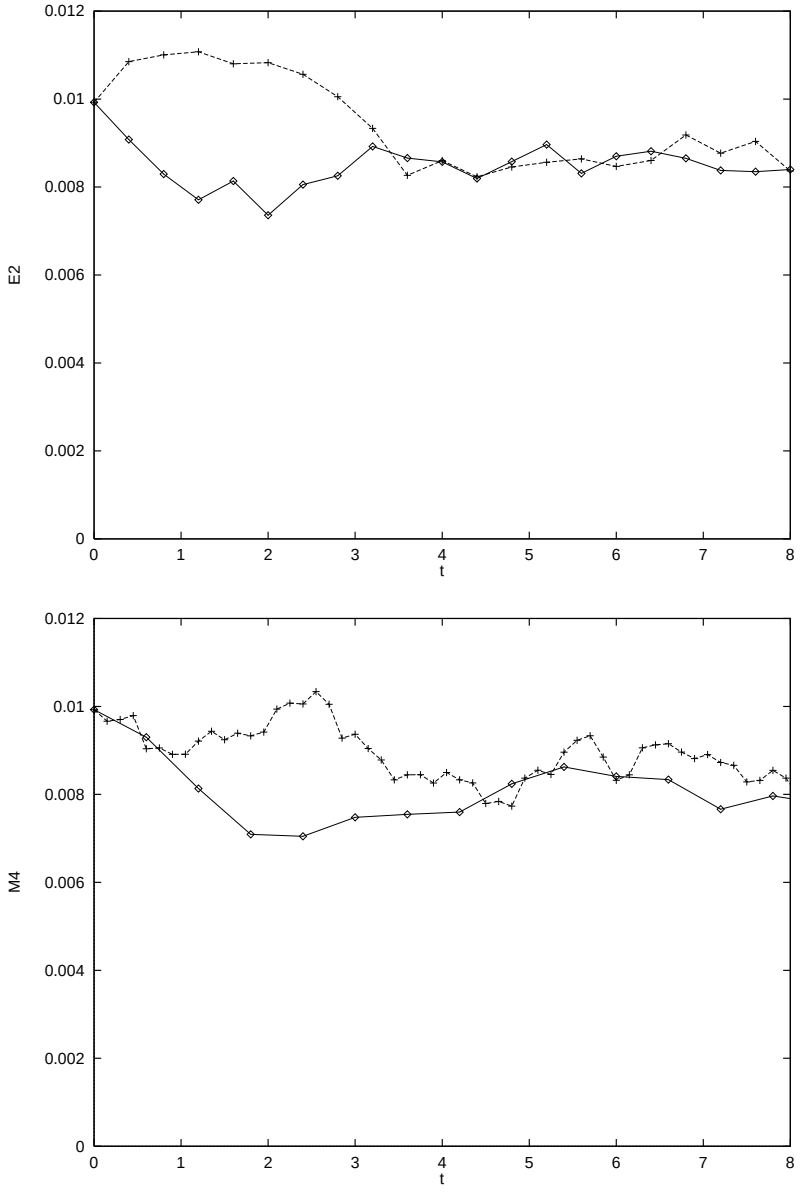

Figure 5: Maxwell molecules: L^2 norm of the error vs time. DSMC (+) and TRMCH ($\diamond$). Top: $\Delta t = 0.4$. Bottom: $\Delta t = 0.15$ (DSMC), $\Delta t = 0.6$ (TRMCH).

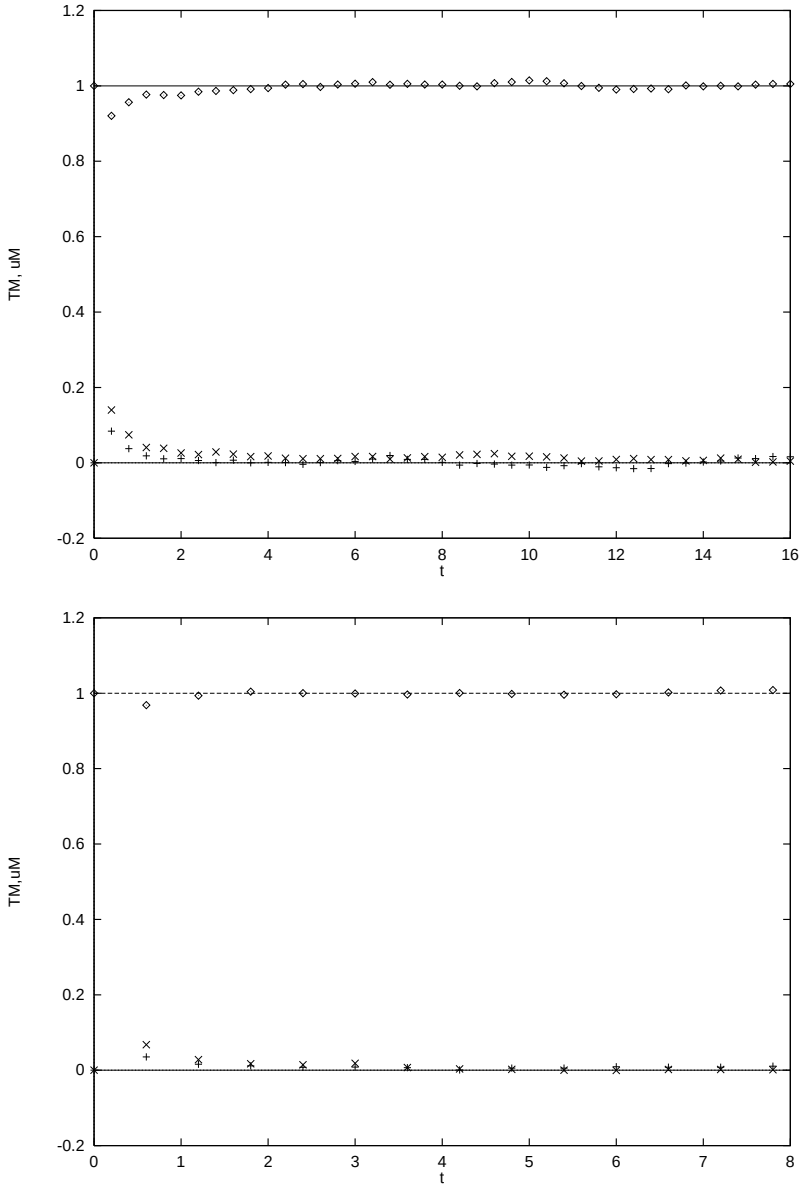

Figure 6: Maxwell molecules: moments of the Maxwellian in the TRMCH method vs time. Temperature T_M ($\diamond$) Velocity $u_{M,x}$ ($\times$) and $u_{M,y}$ ($+$). Top: $\Delta t = 0.4$. Bottom: $\Delta t = 0.6$.

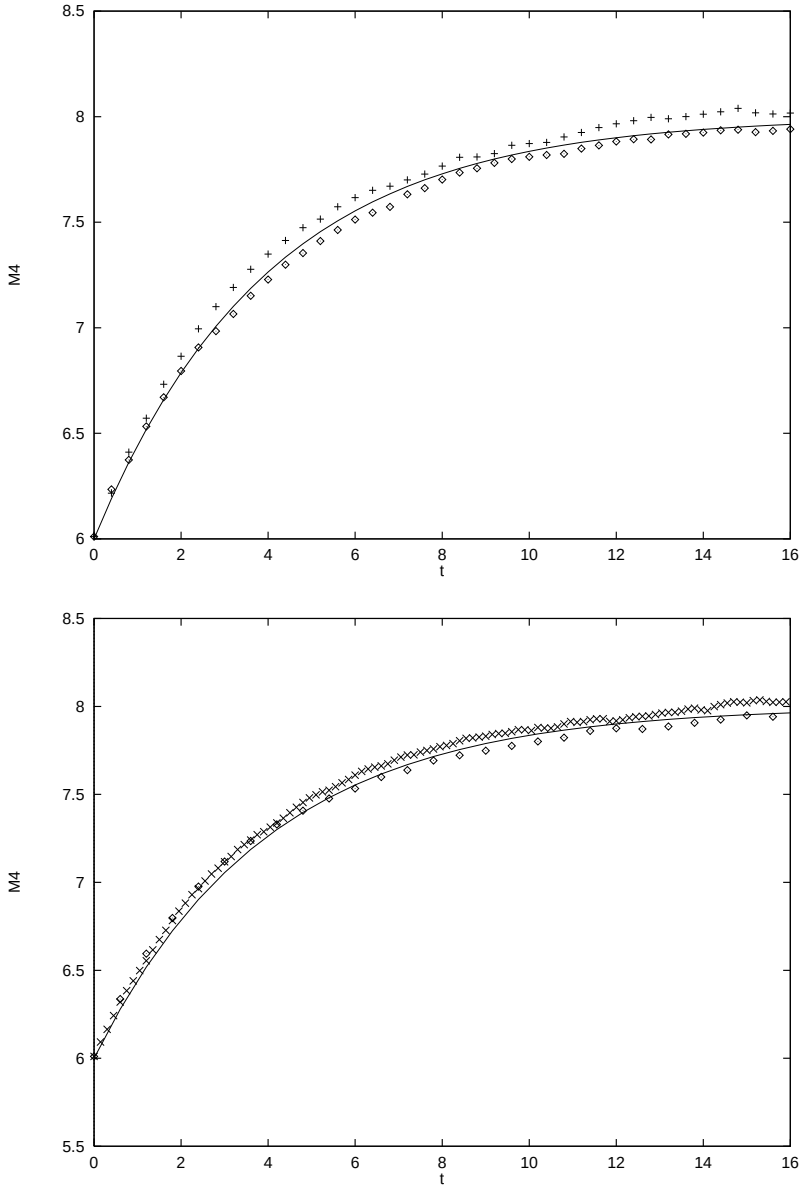

Figure 7: Maxwell molecules: fourth order moment vs time. DSMC (+), TRMCH ($\diamond$), and exact (line) solution. Top: $\Delta t = 0.4$. Bottom: $\Delta t = 0.15$ (DSMC), $\Delta t = 0.6$ (TRMCH).

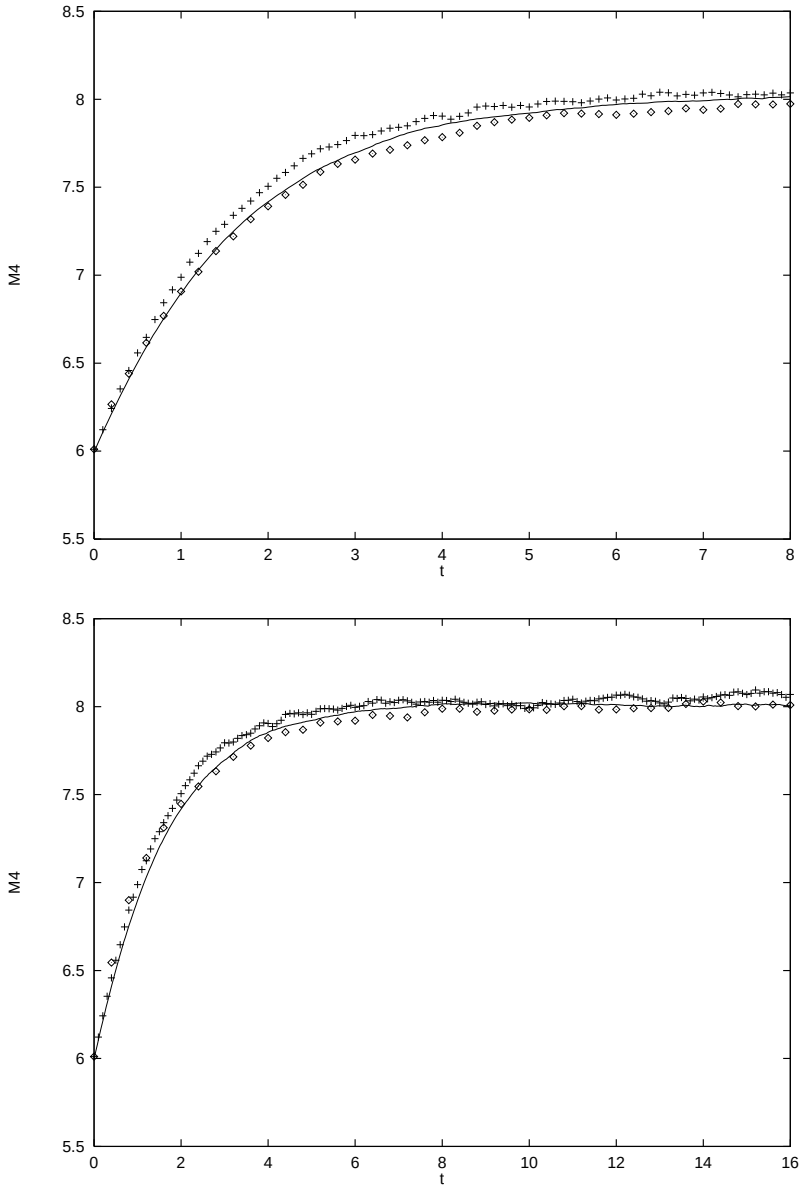

Figure 8: Hard Sphere molecules: fourth order moment vs time. DSMC (+), TRMCH ($\diamond$), and "exact" (line) solution. Top: $\Delta t = 0.1$ for DSMC and $\Delta t = 0.2$ for TRMCH. Bottom: $\Delta t = 0.1$ for DSMC and $\Delta t = 0.4$ for TRMCH.

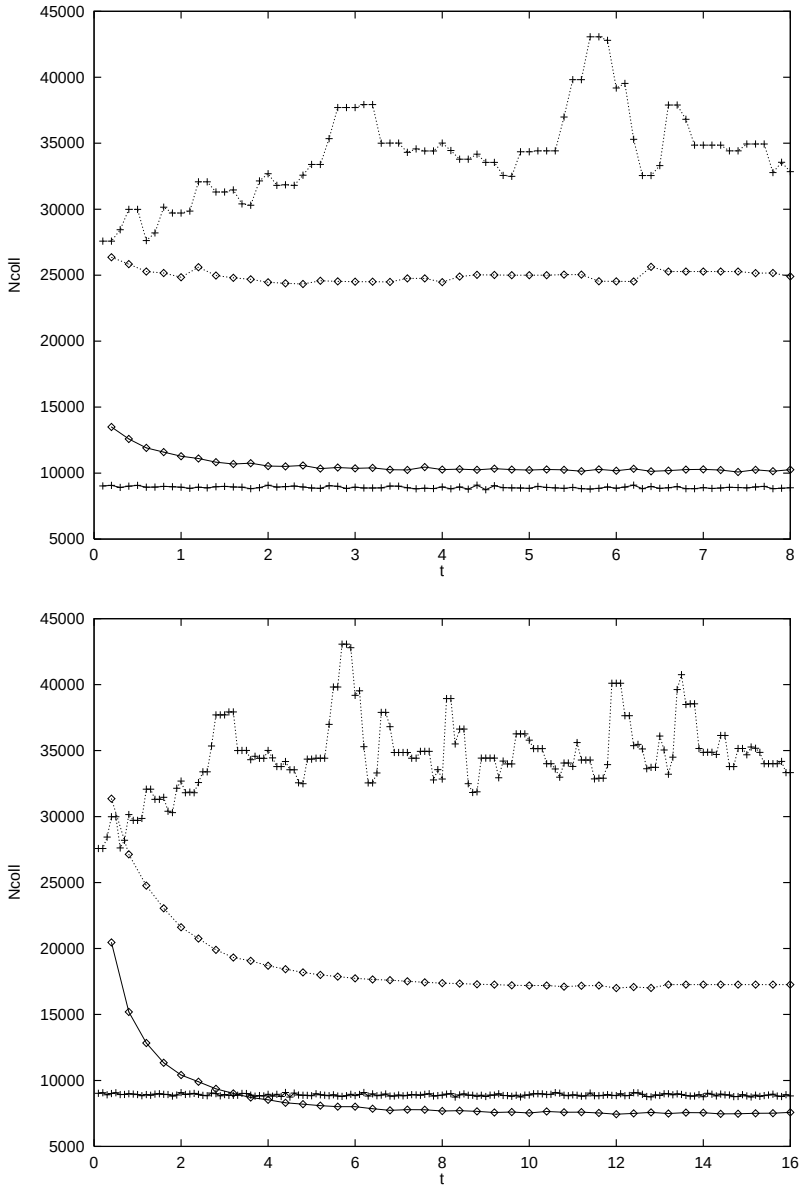

Figure 9: Hard Sphere molecules: number of effective (line) and dummy (dashed line) collisions vs. time. DSMC (+), TRMCH ($\diamond$). Top: $\Delta t = 0.1$ for DSMC and $\Delta t = 0.2$ for TRMCH. Bottom: $\Delta t = 0.1$ for DSMC and $\Delta t = 0.4$ for TRMCH.

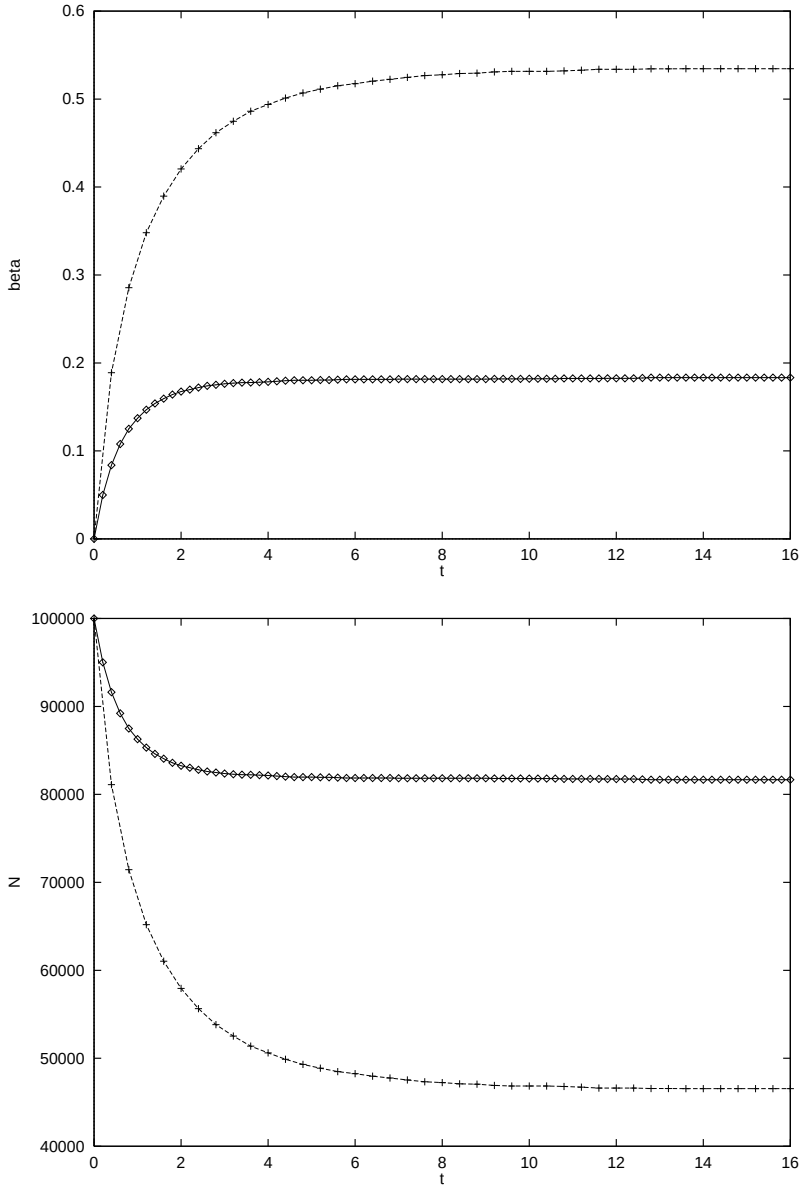

Figure 10: Hard Sphere molecules: value of β^n (top) and number of particles (bottom) vs time for TRMCH. Time step: $\Delta t = 0.2$ ($\diamond$), $\Delta t = 0.4$ (+).